

Supplementary material:

Challenges in modeling the energy balance and melt in the percolation zone of the Greenland ice sheet

Federico COVI,¹ Regine HOCK,^{1,2} Carleen H. REIJMER,³

¹*Geophysical Institute, University of Alaska Fairbanks, Fairbanks, AK, USA*

²*Department of Geoscience, University of Oslo, Oslo, Norway*

³*Institute for Marine and Atmospheric Research, Utrecht University, Utrecht, The Netherlands*

Correspondence: Federico Covi <fcovi@alaska.edu>

Supplementary Tables

Table S1: Modeled melt at Site J for simulations including deep water percolation. (*p.* 2)

Supplementary Figures

Figure S1: Subsurface liquid water content and refreezing at Site J for simulations including deep water percolation. (*p.* 3)

Figure S2: Subsurface temperature difference between model and observations at Site J for simulations including deep water percolation. (*p.* 4)

Figure S3: Subsurface temperature model validation at EKT and Site J for the simulations forced with observed surface temperature ($sim_T_s^{obs}$). (*p.* 5)

Figure S4: Surface energy balance components at Site J for the sim_ref and $sim_T_s^{obs}$ simulations. (*p.* 6)

Supplementary Figures - Model Sensitivity at EKT

Figure S5: Model sensitivity to input forcings at EKT. (*p.* 7)

Figure S6: Model sensitivity to model parameters and parameterizations at EKT. (*p.* 8)

Figure S7: Model sensitivity to shortwave radiation penetration at EKT. (*p.* 9)

Figure S8: Model sensitivity to deep water percolation at EKT. (*p.* 9)

Table S1. Modeled melt (mm w.e.) over the whole study period at Site J for simulations including deep water percolation. Results using different depth of maximum percolation (2.5, 5.0, and 7.5 m) and different percolation probability density functions (UNI, LIN, and NORM) are presented.

	2.5 m	5.0 m	7.5 m
UNI	1017	984	961
LIN	1040	1012	993
NORM	1049	1022	1004

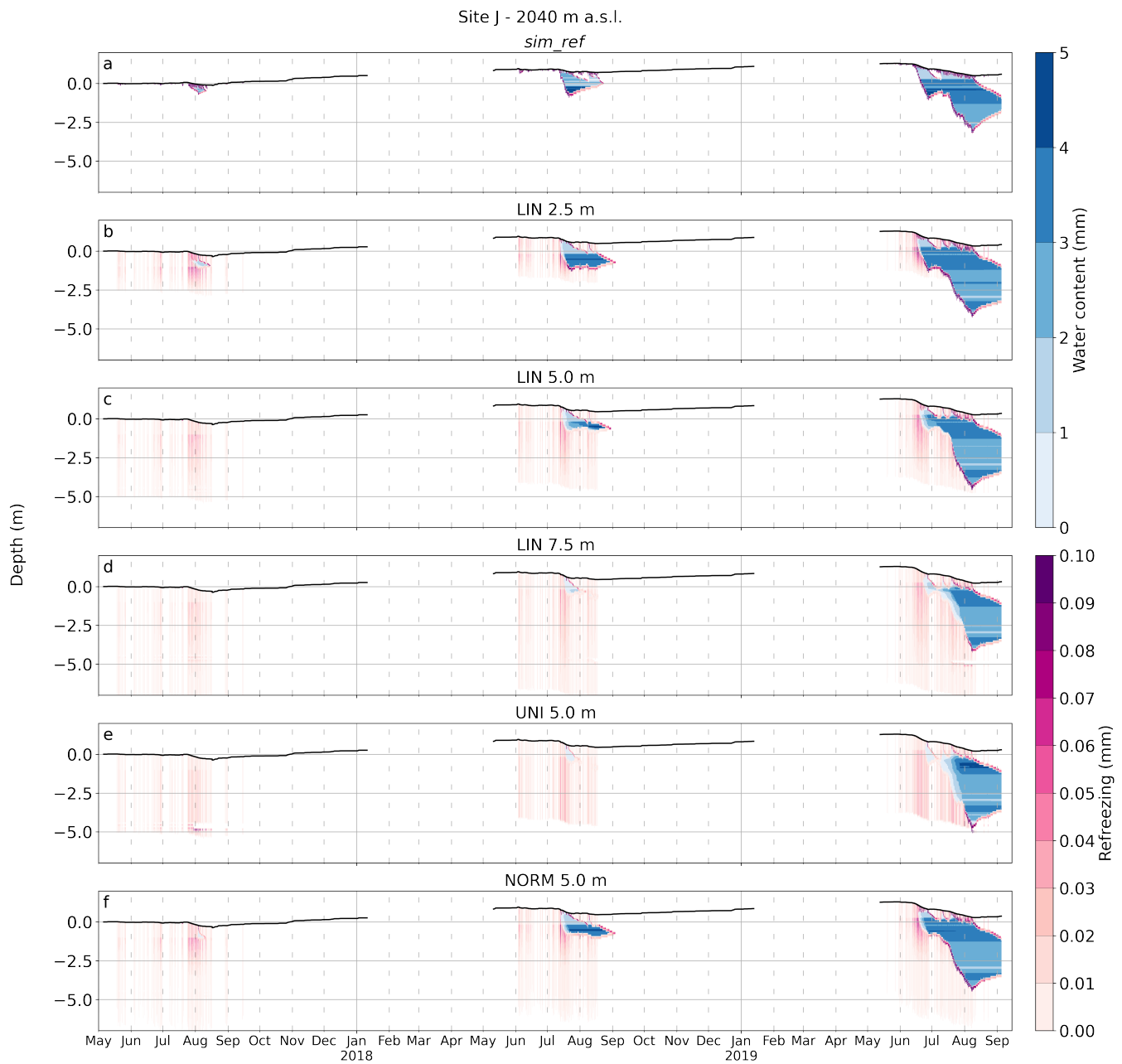


Fig. S1. Hourly subsurface liquid water content and refreezing for simulations including deep water percolation at Site J. Results using different percolation probability density functions and depths of maximum percolation are presented: (a) reference simulation, (b) linear 2.5 m, (c) linear 5.0 m, (d) linear 7.5 m, (e) uniform 5.0 m, and (f) normal law 5.0 m. The simulated surface height is shown as a black line.

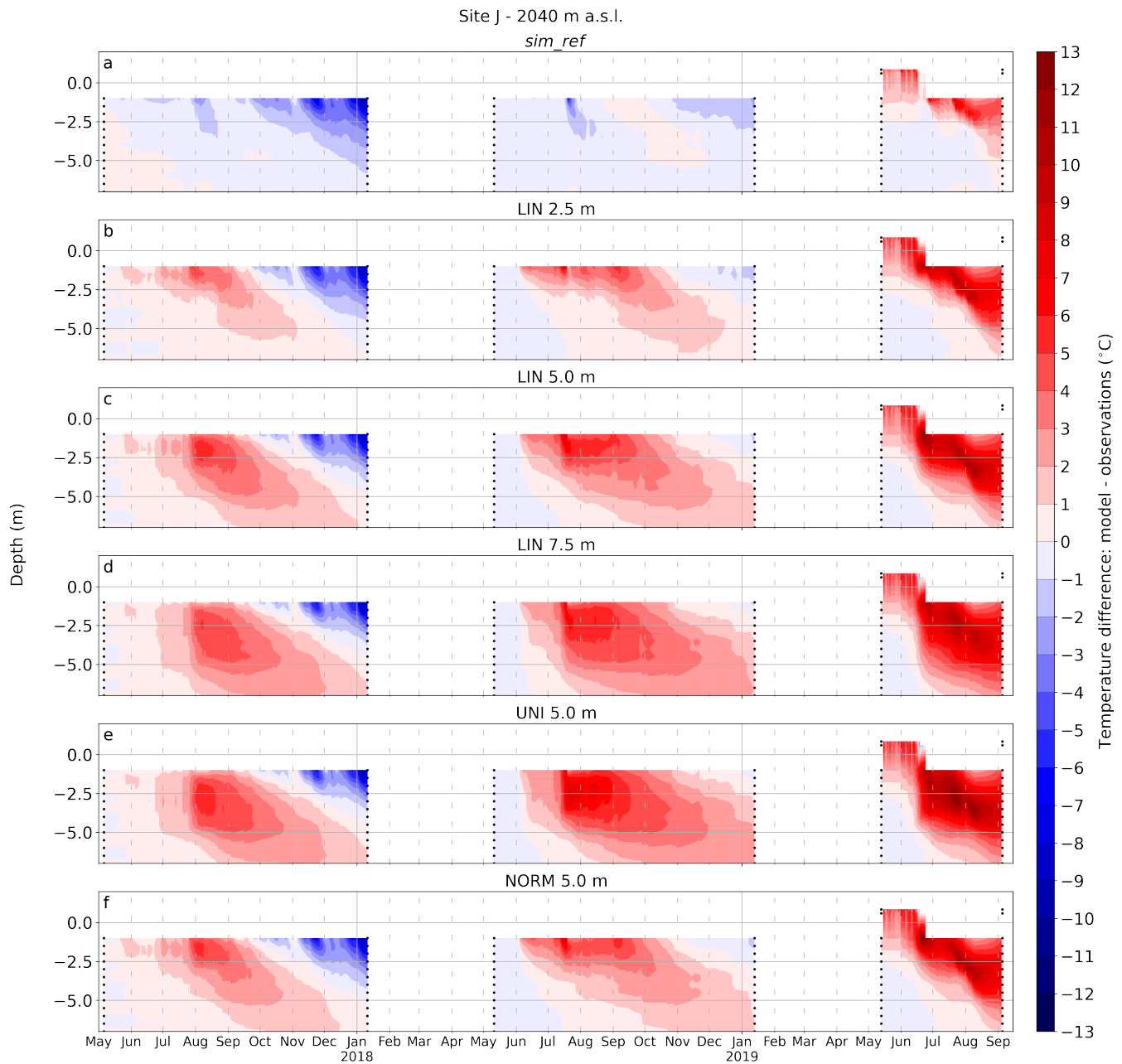


Fig. S2. Hourly subsurface temperature difference between model and observation for simulations including deep water percolation at Site J. Results using different percolation probability density functions and depths of maximum percolation are presented: (a) reference simulation, (b) linear 2.5 m, (c) linear 5.0 m, (d) linear 7.5 m, (e) uniform 5.0 m, and (f) normal law 5.0 m. Black dots indicate the position of the thermistors.

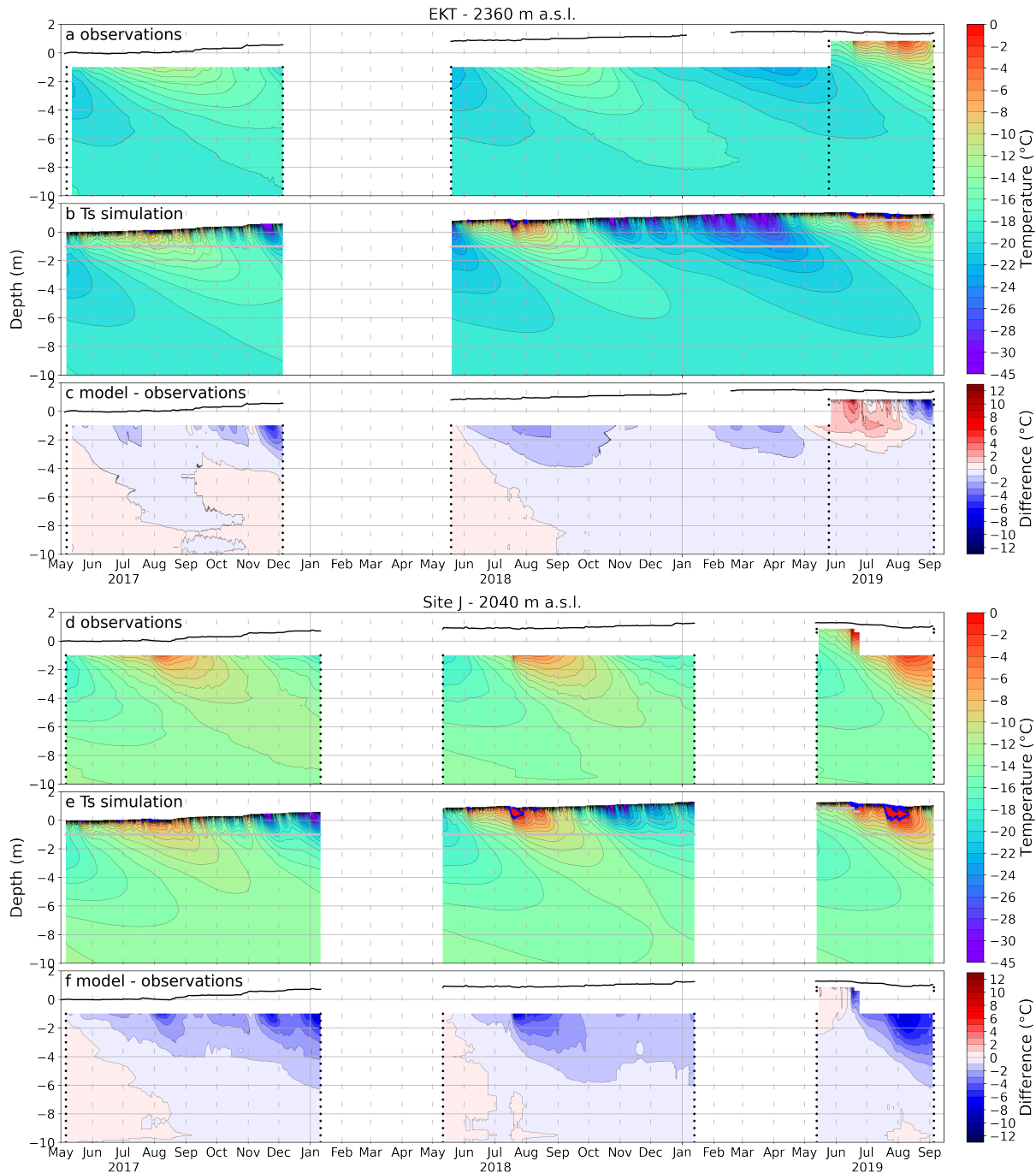


Fig. S3. Hourly measured (a, d), modeled (b, e) subsurface temperatures and their differences (d, f) for the uppermost 10 m between May 2017 and September 2019 at EKT (a–c) and Site J (d–f) for simulations forced with observed surface temperature. Depths are relative to the snow surface on the date of installation in early May 2017. Black lines in (a, c, d, f) mark the evolving surface from the sonic ranger measurements, and the black dots show the position of the thermistors. Blue lines in (b, e) surround the area of subsurface liquid water. Grey lines in (b, e) indicate the depth of the uppermost thermistor. Data from the new thermistors installed in May 2019 are omitted in (a, c, d, f) when the sensors reached the surface or were affected by solar radiation penetration. (Same as Fig. 3 but for simulations forced with observed surface temperature)

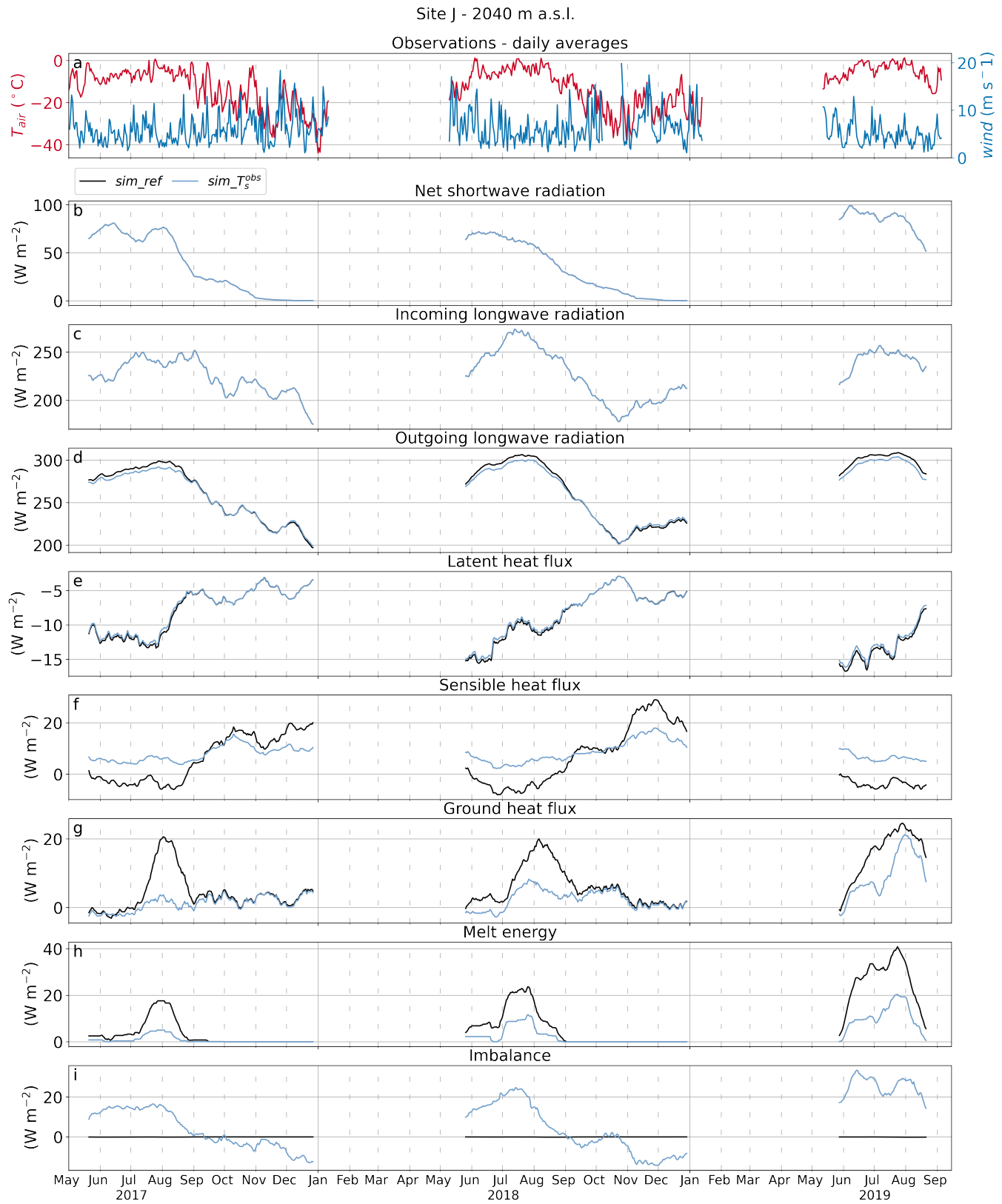


Fig. S4. Daily averages of air temperature and wind speed and 30-day rolling averages of surface energy balance components for *sim_ref* and *sim_T_s^{obs}* simulations at Site J: (a) air temperature and wind speed, (b) net shortwave radiation, (c) incoming longwave radiation, (d) outgoing longwave radiation, (e) latent heat flux, (f) sensible heat flux, (g) ground heat flux, (h) energy available for melt, and (i) surface energy balance residual. (Same as Fig. 11 but for Site J)

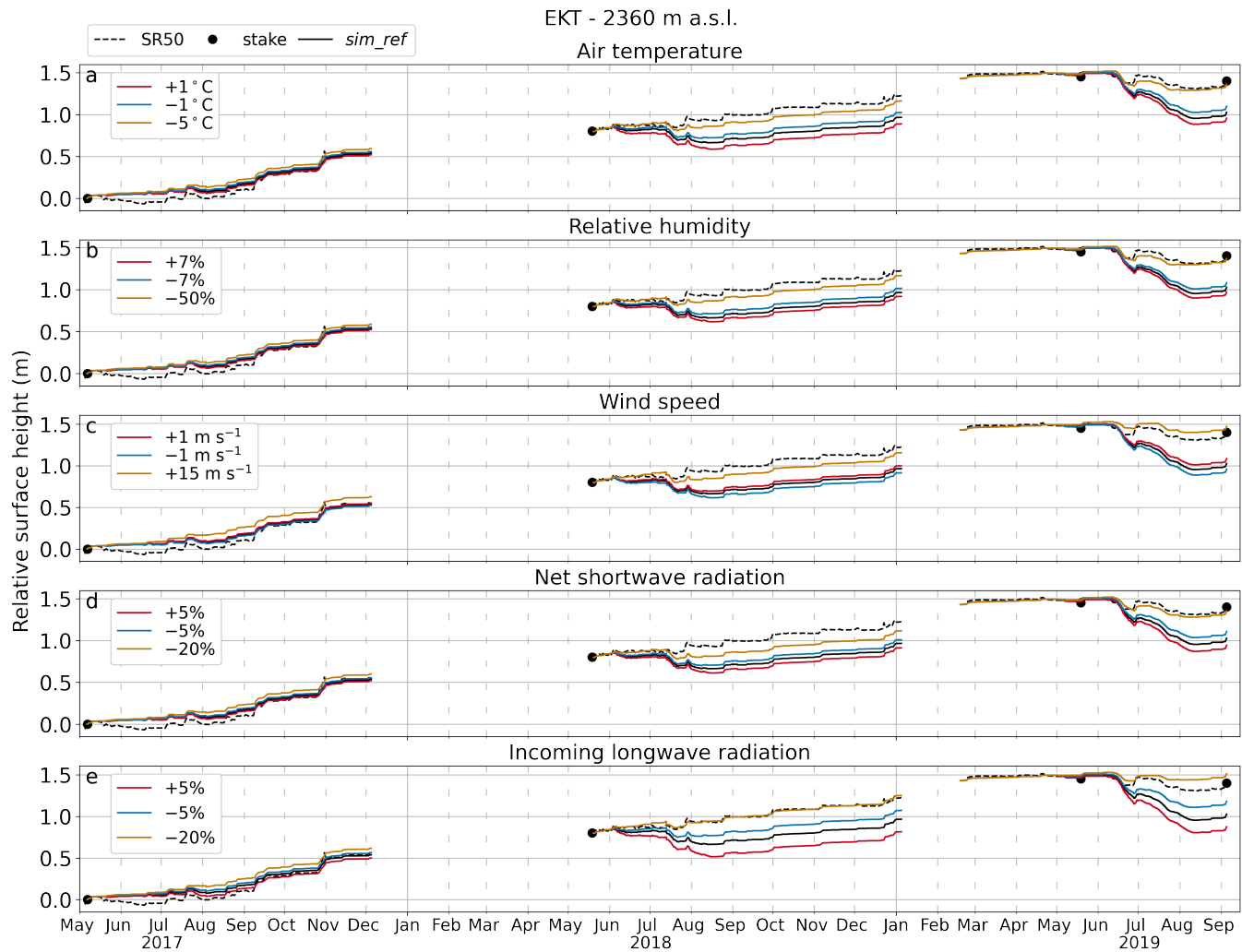


Fig. S5. Modeled hourly relative surface height compared to measurements from AWS sonic ranger (SR50) and ablation stake at EKT for simulations with different model forcings: (a) air temperature, (b) relative humidity, (c) wind speed, (d) net shortwave radiation, and (e) incoming longwave radiation. (Same as Fig. 4 but for EKT)

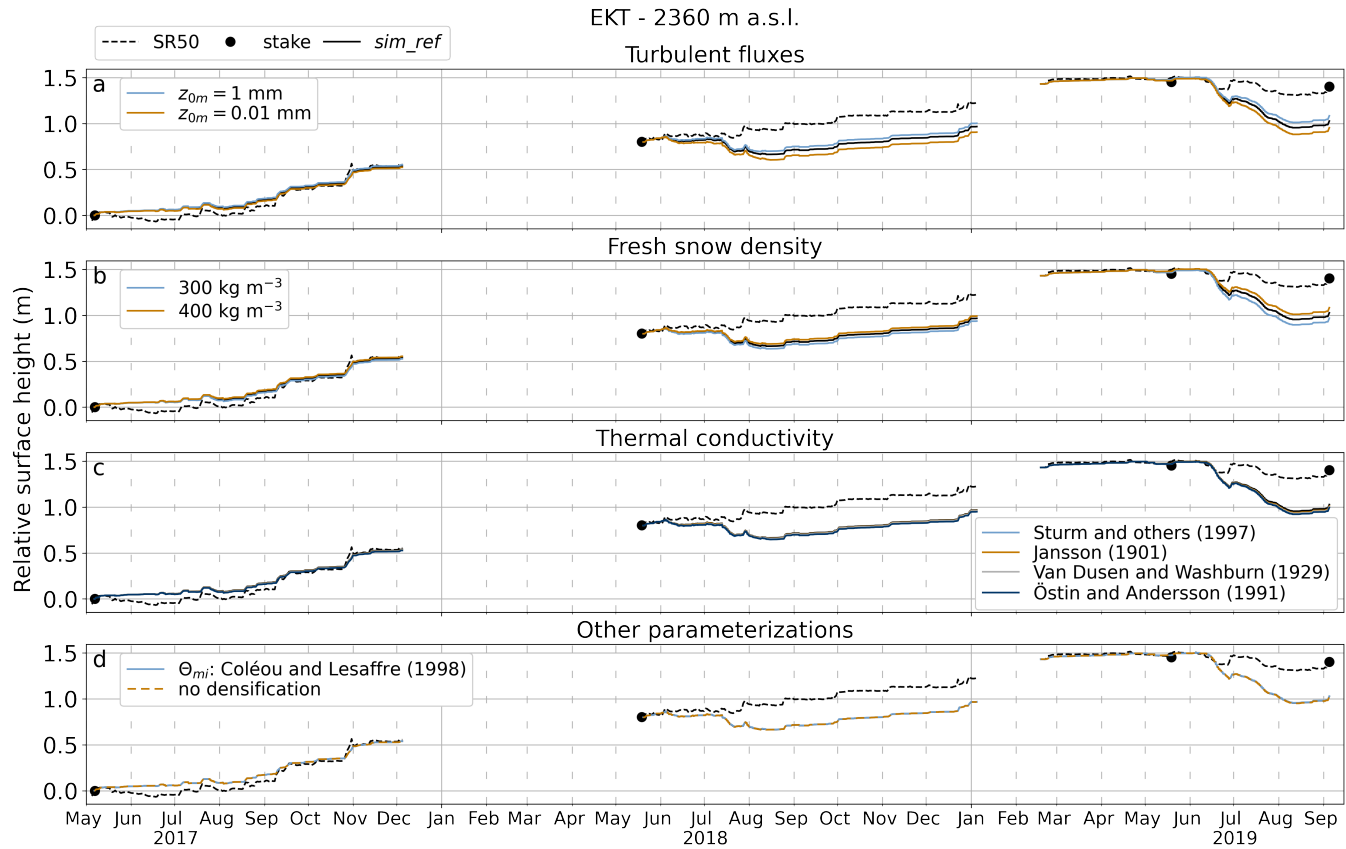


Fig. S6. Modeled hourly relative surface height compared to measurements from AWS sonic ranger (SR50) and ablation stake at EKT for simulations with different model parameters and parameterizations: (a) turbulent fluxes, (b) fresh snow density, (c) thermal conductivity, and (d) densification and irreducible water content (Θ_{mi}) parameterizations. (Same as Fig. 5 but for EKT)

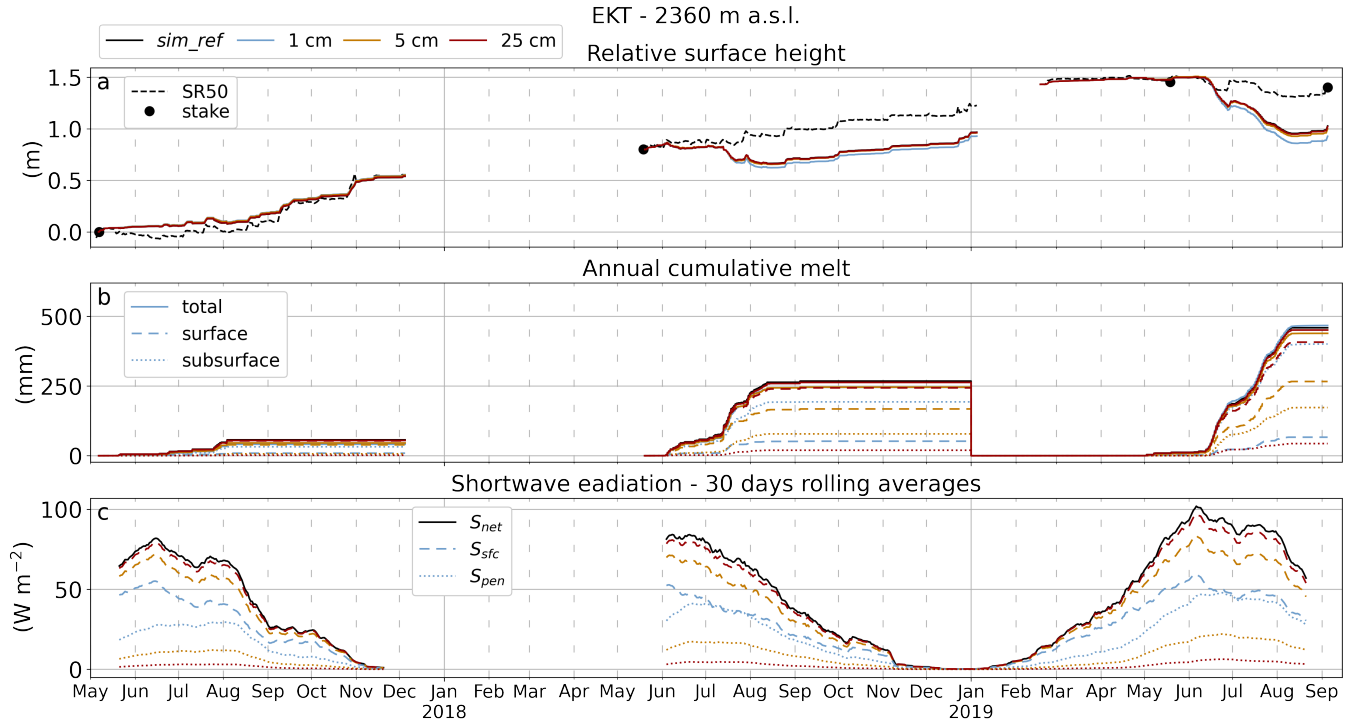


Fig. S7. (a) hourly relative surface height, (b) annual cumulative total, surface, and subsurface melt, and (c) 30-day rolling average of shortwave radiation components (S_{net} , S_{sfc} , and S_{pen}) for simulations including radiation penetration at EKT. Results using different fictitious surface layer thicknesses are presented: 1 cm in cyan, 5 cm in orange, and 25 cm in red. Reference simulation in dashed black and observations in solid black. (Same as Fig. 6 but for EKT)

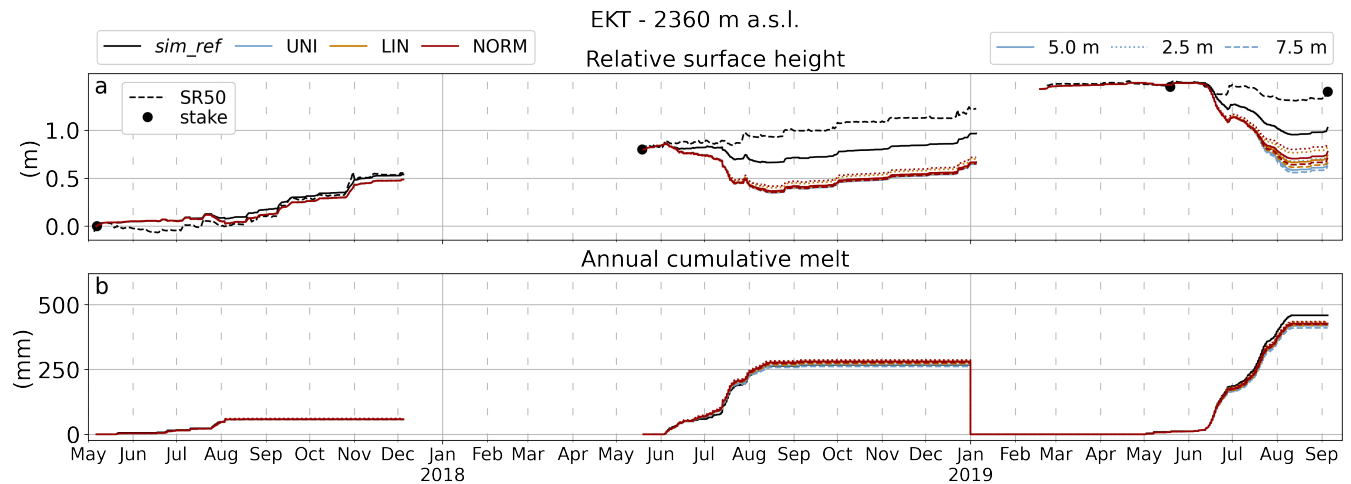


Fig. S8. (a) hourly relative surface height and (b) annual cumulative melt for simulations including deep water percolation at EKT. Results using different percolation probability density functions (UNI in cyan, LIN in orange, and NORM in red) and depth of maximum percolation (2.5 m dotted, 5.0 m solid, and 7.5 m dashed) are presented. Reference simulation in solid black and observations in dashed black. (Same as Fig. 8 but for EKT)